Simulation and Measurement of Nonlinear Behavior in a High-Power Test Cell

Gerald Harvey and Anthony Gachagan

I. Introduction

High-power ultrasonic systems are commonly used in many applications such as food processing [1], water treatment [2], microbe inactivation [3], cleaning [4], and cutting [5]. It is a particularly application-focused technology although recently a large degree of interest has developed in the research community pertaining to more efficient systems [6], in-process applications [7], and system qualification methods [8]. At the heart of many of these applications is the generation of cavitation within the high-power cell [9]. The phenomenon of cavitation produces a series of dramatic effects that have a powerful effect on the liquid media in which it is induced, effects such as extremely high local temperatures (3000 K) and pressures (10 GPa) [10]. These effects create a local environment that can directly influence chemical reactions, material properties, and even chemical structures [11]. Cavitation itself is likely to occur within regions of a test cell that exhibit higher intensities. Therefore, accurate knowledge of spatial pressure distribution within such cells can be valuable when attempting to optimize the location of such regions.

It is often assumed that the propagation of ultrasound is a linear process, i.e., that the traveling wave has constant velocity, c_o, and so retains its shape as it travels through the load medium. However, when higher amplitudes of input signal are employed, it is often not difficult to generate sufficient pressures in a liquid medium to complicate linear models, especially as the wavelength decreases with input remaining constant. When these higher pressures are achieved, nonlinear effects will become apparent and the profile of the wave will be subject to certain changes. The compressional phase of the wave will cause an increase in the local density of the medium through which it travels, and given that the velocity of sound is dependent on the momentary value of density, points in the wave of greater amplitude will travel faster than those of lesser amplitude. Thus, the positive cycle of an originally sinusoidal plane wave becomes increasingly steeper over the course of its propagation, as illustrated graphically in Fig. 1. Because of this distortion of the wavefront in the time domain, the frequency spectrum of the wave will, as a consequence, also be altered. Spectral components, or harmonics, at integer multiples of the original frequency will become apparent in the Fourier transform of the temporal information. Finally, this steepening process leads to the formation of pressure discontinuities, known as shock fronts, which manifest themselves as vertical tangents in the waveform, i.e., the waveform transforms into a sawtooth profile, shown in Fig. 1(d).

This phenomenon has generated a great deal of interest over the past 50 years or so, spawning a variety of practical applications in the process, e.g., medical ultrasound scanners using tissue harmonic imaging [12]. The effect harmonic presence can have on a field profile can be quite pronounced, particularly when comparison is made to the original linear field. Fig. 2 illustrates the simulated differences (PZFlex, Weidlinger Associates, Mountain View, CA) in field profiles which can be introduced when a sample high-power system transitions from linear to nonlinear behavior (up to the 4th harmonic with a value of 30 dB). The vessel shown is cylindrical in nature, 6.5 wavelengths long and 1.5 wide at an operating frequency of 40 kHz. The length is exaggerated slightly here to more clearly represent the changes that can occur. From the figure, it is evident that the spatial location and amplitude of peak pressure regions differ significantly from the linear and nonlinear cases in both the axial and transverse direc-

Manuscript received July 7, 2010; accepted February 1, 2011. The authors acknowledge funding for this research through EPSRC projects EP/F016522/1 and EP/N17928/01.

G. Harvey is with Weidlinger Associates, Glasgow, Scotland.

A. Gachagan is with the Centre for Ultrasonic Engineering, Department of Electronic & Electrical Engineering, Glasgow, Scotland (e-mail: a.gachagan@eee.strath.ac.uk).

Digital Object Identifier 10.1109/TUFFC.2011.1873

In effect, the quantity B/A will vary depending on the temperature, hydrostatic pressure, and density of the medium through which a finite amplitude sound wave is propagating. Examples of this quantity for two common load media are as follows; distilled water has a ratio B/A = 5 and air has B/A = 0.4, both calculated at a temperature of 20°C. The higher the ratio, the more likely a medium is to generate nonlinear effects.

B. KZK Equation

The KZK equation accounts for the combined effects of diffraction, absorption, and nonlinearity in directional sound beams. Eq. (3) represents the nonlinear parabolic KZK equation [14]:

$$\frac{\partial^2 p}{\partial z\,\partial t} = \frac{c_o}{2}\left(\frac{\partial^2}{\partial x^2} + \frac{\partial^2}{\partial y^2}\right)p - \frac{\delta}{2c_o^3}\frac{\partial^3 p}{\partial t^3} - \frac{\beta}{2\rho_o c_o^3}\frac{\partial^2 p^2}{\partial t^2}. \quad (3)$$

The first term on the right-hand side describes the effects of diffraction where the expression in parentheses is the transverse Laplacian operator, $\nabla_\perp^2$, which is equivalent to

$$\nabla_\perp^2 = \nabla^2 - \frac{\partial^2}{\partial z^2}. \quad (4)$$

The second term describes the effects of dissipation on a traveling wave. Finally, the third term describes nonlinear effects on the evolution of a propagating sound wave.

The KZK model assumes that the acoustic energy propagates in a fairly narrow beam close to the source axis up to around 20° of the z-axis in the far field. Moreover, the approximation is valid for field points that are beyond a few source radii and regions that are not too close to the source plane. The assumption to be satisfied for a circular, piston-like source of radius a and wavenumber k, is that $ka \gg 1$, hence ensuring that the beam is reasonably directional, the angular spectrum is narrow, and, therefore, wavefronts are quasi-planar [2], [4], [15]. The KZK equation is the most widely used model for describing all three effects on the development of a traveling acoustic wave in a homogenous medium; solutions in the time domain and spectral domain have been developed [16], [17].

C. Analytical Approach

Because of the KZK model's ability to describe the evolution of a traveling wave distorted by the effects of diffraction, absorption, and nonlinearity within certain limitations, several computer algorithms have been proposed to solve the KZK equation numerically. The first approach developed was a frequency domain method, often called the spectral technique, formulated by Aanonsen et al. [17]. The KZK equation can be solved in the frequency domain for monochromatic or tone burst signals by using a finite difference scheme to propagate the wave forward in small steps. Essentially, the pressure wave can be written in terms of Fourier components consisting of the fundamental and its harmonics, truncated at the Nth harmonic to reduce calculation burden, and then substituted into the KZK equation. This enables a set of coupled equations to be derived that allows each harmonic at a grid point in the (x, y) plane at a distance $z + \Delta z$ to be written in terms of the harmonic amplitudes at z. The computational procedure for solving these equations can become very time intensive because the calculation of each harmonic, for a distorted waveform involving N harmonics, will involve N^2 multiplications at each grid point. This problem is further compounded if frequency dependent absorption and strongly focused beams must be accounted for in the prediction. Furthermore, if the source excitation comprises transient signals, or pulses, then a sufficiently low pulse repetition rate is required to ensure that adjacent pulses in the sequence do not overlap as a result of potential lengthening in duration caused by absorption and nonlinearity otherwise, the computational burden can be increased by an order of 100.

The spectral approach was followed by a more generic technique in the time domain proposed by Hamilton and Lee [16]. Solving each term in the KZK model in the temporal domain significantly reduces computational demands compared with frequency domain solutions, primarily because the nonlinear term can be solved with a computational time proportional to N rather than N^2. In addition, time-domain solutions do not require implementation of Fourier transforms. A marching scheme based on evaluating each of the effects individually was used as the basis for this solution.

D. Finite Element Approach

Despite the excellent agreement achieved between results from experiment and models based on the KZK equation, these algorithms remain too idealized for application to more complicated problems involving scattering, cavitation, and medium inhomogeneities. A more useful approach for modeling nonlinear propagation in a load is to implement an incrementally linear solution to the governing elasticity equations [18]. In effect, for transient phenomena, this process involves advancing a solution in time by small, discrete steps and modifying material properties according to the new state of the material. These time increments are short enough that the solution is linear over each step, ensuring that wave nonlinearities are well-modeled by the incrementally linear approach. This technique, i.e., the constant repetition of simple calculations, is ideally suited to numerical solution using FEA code; specifically, the PZFlex package has been used in this work. The code implements a model based on [18]

$$p = p_o + \rho_o c_o^2 \left[\frac{\Delta S_o}{S_o} + \frac{B/A}{2}\left(\frac{\Delta S_o}{S_o}\right)^2 + \right. \quad (5)$$

where p is the change in pressure, p_o is the ambient pressure, ρ is the change in density and ρ_o is the ambient density

This allows a selected region of the grid, which is nonpiezoelectric in nature, to be allocated material properties that support nonlinear propagation under the correct conditions, i.e., sucient pressure amplitudes and/or distance from source. Importantly this allows nonlinear behavior to be simulated by an FE approach.

The large majority of the literature on nonlinear propagation and simulation techniques focuses on the use of ultrasound in medical applications that operate at relatively high frequencies (2 to 10 MHz). At these frequencies, sufcient pressures for harmonic creation are easy to generate at small input levels, where pressure is proportional to particle displacement (or velocity) and frequency as such

$$P \quad {}_o c_o S \; Y, \tag{6}$$

where ξ = particle displacement.

In addition, the associated reduction in wavelength allows for large propagation distances, in terms of number of wavelengths, over a small range. Therefore, in water and biological samples, it is fairly easy for the evolution of a pressure wave to deviate from its pure sinusoidal form. However, at the much lower frequencies that favor the generation of cavitation (20 to 100 kHz), it is not so easy to generate the pressure levels, or transmission distance, in the load required for the initiation of nonlinear behavior, with the obvious exception of sonar.

This creates an interesting scenario when investigating the pressure elds generated in the test vessels used prevalently in industrial processing applications, in that it may be possible to stimulate cavitation while the system effectively remains in the linear regime. Indeed, it is not unreasonable to postulate that the generation of harmonics in this situation may be more of a hindrance when attempting to maximize cavitational events because the fundamental frequency leaks energy to the higher frequencies.

It is often assumed that because of the high input levels associated with ultrasound in many process and ultrasonic cleaning applications, nonlinear waveforms will be readily generated. The presence of harmonics caused by nonlinear propagation can have a profound impact on the eld prole, causing it to deviate from the linear prole. Therefore, for the accurate characterization of such acoustic elds, it is important that nonlinear eects, if any are well-represented. Simulation of these eects in the ultrasonic system is possible through inclusion of a transmission load that supports nonlinear eects in the model.

Because PZflex cannot represent piezoelectric nonlinearities caused by high input voltages, any harmonics produced in the load medium would arise from acoustic activity simulated within the vessel itself. However, in practice, equipment and device nonlinearities may exist and contribute to the acoustic eld. It should be noted that these eects are separate from the nonlinearities associated with the onset of cavitation, both inertial and non-inertial, where bubble oscillations can generate harmonics and sub-harmonics of the fundamental frequency and where bubble implosions can produce broadband acoustic pulses. These are also not represented directly by PZflex.

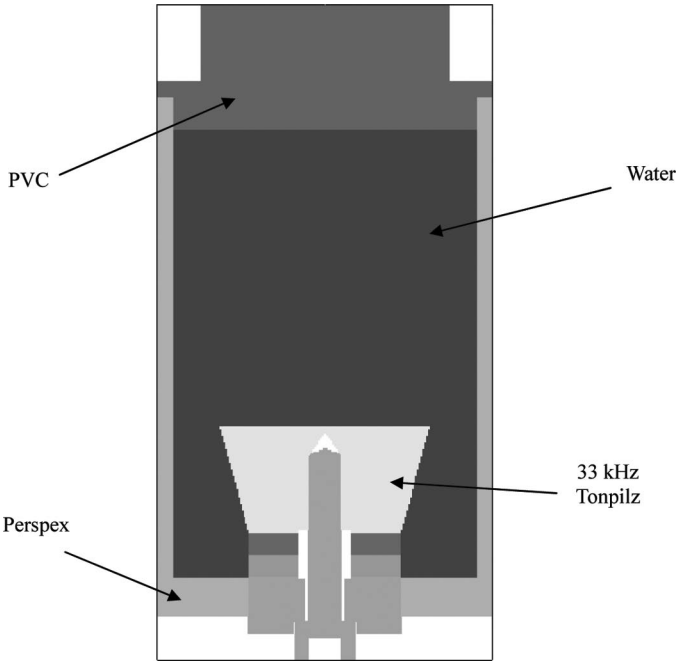

Fig. 3. Finite element representation of the Tonpilz transducer featured in a high-power cylindrical test cell for nonlinear propagation simulation.

TABLE I. L kD U FE C
R E W 33-H 40-H
S.

Aspect	33-kHz size (mm)	40-kHz size (mm)
Cell outer diameter	100	100
Cell wall thickness	5	5
PVC xture thickness	31	31
PVC xture inner diameter	77	70
Perspex holder thickness	10.5	18.4
Overall length	169	129
Tonpilz front face diameter	63	50
Wavelength in water	45.5	37.5

III. M

To generate classical nonlinear eects at low frequencies within a conventional high-power test cell, an input of several hundred volts is required. Given this, it is reasonable to postulate that cavitational eects will occur before the system becomes nonlinear. Therefore, a sample cylindrical test cell, shown in Fig. 3 with details in Table I, was designed and built to investigate this possibility The system is powered by either one of two commercially available Tonpilz transducers (Morgan Electro Ceramics, Southampton, England) at 33 and 40 kHz. It is important

the transmission device or harmonics generated in the load. This will be investigated in the following sections.

B. Transmission Device

Commonly with piezoelectric devices, harmonics are present at odd integer multiples of the fundamental thickness mode, where this mode is a half-wavelength longitudinal resonance of the device thickness, hence

$$f_n \quad \frac{nV_t}{2d_t}, \tag{7}$$

where V_t is the velocity of sound in the piezoelectric material, d_t is the thickness, and n is an integer wavenumber. Given this, n takes the values 1, 3, 5, etc., and leads to nulls at even integer harmonics. However, if input levels are large enough, a degree of nonlinearity can be induced in the piezoelectric material and facilitate the generation of even harmonics. Measurement of these harmonics is a reliable technique to determine the linearity of a device at a given input level.

Device linearity is traditionally evaluated through the detection of harmonics by a hydrophone positioned along the acoustic axis. The ultrasonic device is driven at its electrical resonance frequency either continuous wave (CW) or pseudo-CW in water, with steadily increasing voltage levels using a power amplier and an arbitrary signal generator. It should also be noted that maintaining the required free-eld conditions for this type of investigation can be problematic because of the reections from the tank walls.

The signal captured by the hydrophone is transformed into the spectral domain and analyzed for the presence of harmonics. In addition, the temporal waveform can be scrutinized for any variances between maximum positive and negative pressure values, because this also indicative of nonlinear behavior. For this investigation, the previously characterized drive equipment was again used in conjunction with a Bruel & Kjer 8103 low-frequency hydrophone (Naerum, Denmark). The location of the hydrophone within the eld is crucial to the accuracy of the measurement. It should be situated in the far eld to ensure it is not in a pressure null, which are common in the near-eld. Notwithstanding, it should not be placed in the extremities of the far-eld because the increased propagation distance from the source can cause nonlinear behavior. This makes it dicult to distinguish between harmonics generated from the device and those created through conventional means. Indeed, this proved to be the case in practice and an alternative arrangement was devised for such low-frequency devices.

The solution is to simply remove the potential for the transmission load to generate harmonics and evaluate the device in an air channel. Because it is extremely dicult to generate conventional nonlinear eects in air using ultrasound because of the attenuation at these frequencies, any harmonics detected in the spectral prole must be due to the device. Again, adherence to placing the hydrophone in the far-eld must be maintained. This arrangement also negates the diculties associated with attempting to maintain free-eld conditions in a water tank.

An alternative hydrophone better suited to air-coupled ultrasound was employed for the new set-up. A PVDF membrane device with an active area of 5 mm in diameter, complete with pre-amplication electronics, was substituted for the Bruel & Kjer probe. The membrane device was fabricated in-house using the techniques described in [19]. The hydrophone was placed 120 mm from the front face for the 33- and 40-kHz Tonpilz transducers. Importantly, the position of the PVDF device remained perpendicular to the acoustic axis to prevent any additional modes from being excited in the PVDF substrate, which these devices are particularly susceptible to at lower frequencies [19].

Each device was excited at its electrical resonance frequency for maximum transmission eciency with an initial signal of 10 Vpp (with no power amplier). Figs. 6(a) and 6(b) show the comparison between FE and experiment for both Tonpilz devices; the validity of these models has been established previously in [20]. The amplied signal from the hydrophone is connected directly to the oscilloscope, where spectral analysis is instantly available through the FFT function. Figs. 7 and 8 show the spectral content of the received signal from the PVDF membrane hydrophone for the 33- and 40-kHz devices, respectively. From the 33-kHz device, it is clear that a signicant 2nd harmonic of 33 dB at 64.7 kHz is detected, even at these relatively low input levels in an air environment. This is echoed in the result for the 40-kHz device, where the 2nd harmonic is slightly larger at 28 dB for a frequency of 80.2 kHz. An extended FFT for both devices shows that higher harmonics are present, up to the 5th, but at reduced amplitudes.

This result demonstrates that these devices are nonlinear even at low input signal levels. Indeed, when the power amplier was utilized with the arrangement to increase input voltage, the amplitude of the 2nd harmonic was seen to increase proportionally with the fundamental component. A search of the literature has failed to produce any previous evidence of this type of behavior being inherent in Tonpilz devices, therefore further investigation of this characteristic was warranted. The laser vibrometer facility provides an excellent opportunity to conrm, and potentially expand upon, the results from the initial hydrophone evaluation.

C. Evaluation by Surface Displacement Measurement

A Polytec OFV-3001 laser scanning vibrometer (Polytec GmbH, Waldbronn, Germany) and associated software [21] was used throughout this work. The laser vibrometer eciently quanties the surface displacement of a vibrating aperture through the principle of interferometry. Through unconventional application of this established technique, it is possible to analyze the spectral content of an aperture velocity function for any evidence of harmonic

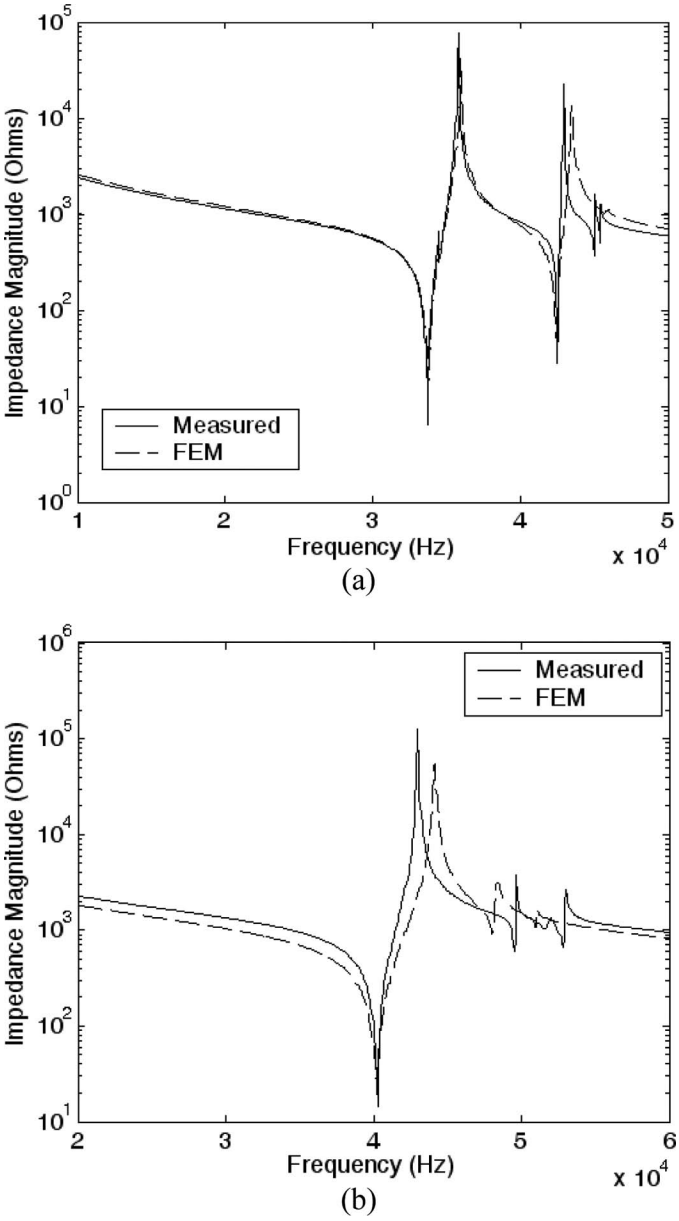

Fig. 6. Measured and simulated electrical impedance proles for the (a) 33-kHz and (b) 40-kHz Tonpilz devices.

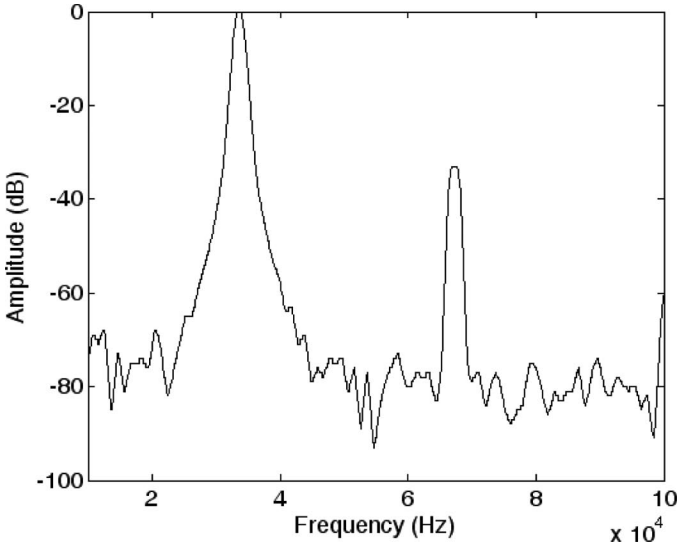

Fig. 7. Frequency spectrum of the received signal from the PVDF membrane hydrophone positioned 120 mm from the 33-kHz Tonpilz device radiating into an air channel.

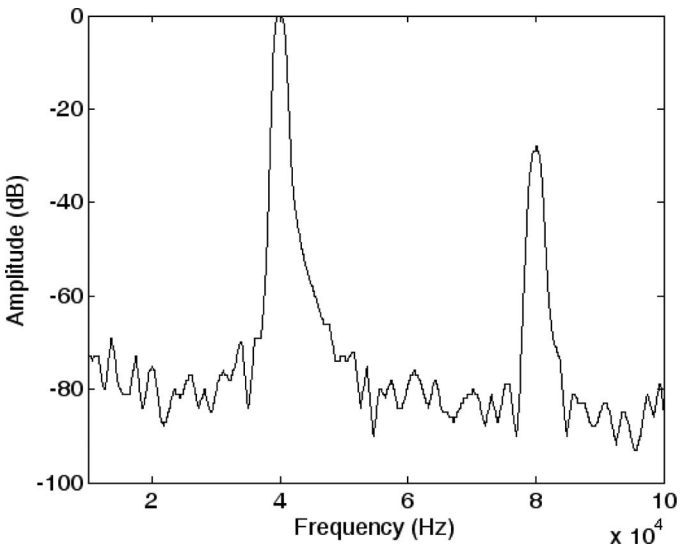

Fig. 8. Frequency spectrum of the received signal from the PVDF membrane hydrophone positioned 120 mm from the 40-kHz Tonpilz device radiating into an air channel.

content. Therefore, by measuring the particle velocity (i.e., the front face velocity) or the front face displacement and applying a FFT, it is possible to condently state whether a device is linear. This technique was applied to both the 33-kHz and the 40-kHz Tonpilz devices.

There are two measurement options available for applying this technique using the laser vibrometer; a single spot measurement and a complete scan of the vibrating aperture. The latter of the two is detailed in this section because of its completeness and similarity to the measurement taken with the hydrophone, in that the entire surface contributes to the pressure eld. Given this, the FFT taken is, in fact, an FFT of the average surface motion for all points recorded by the vibrometer. This provides a more accurate result with a higher SNR than the single spot inspection.

Once again, both transducers were driven under the conditions outlined earlier in this section, with the same drive equipment. It should be noted that the inclusion of the power amplier for higher drive voltages is possible with the vibrometer system. The FFT for the 33- and 40-kHz transducers are shown in Fig. 9 and Fig. 10, respectively. The 2nd harmonics are clearly evident in both gures, located at 67.4 kHz with amplitude of 34 dB for the 33-kHz device, and 80.2 kHz with amplitude of 31 dB for the 40-kHz device. Importantly, these values correspond well with those obtained through traditional linearity evaluation methods using the hydrophone.

In addition to providing evidence of device nonlinearity through analysis of the spectral content of the front face

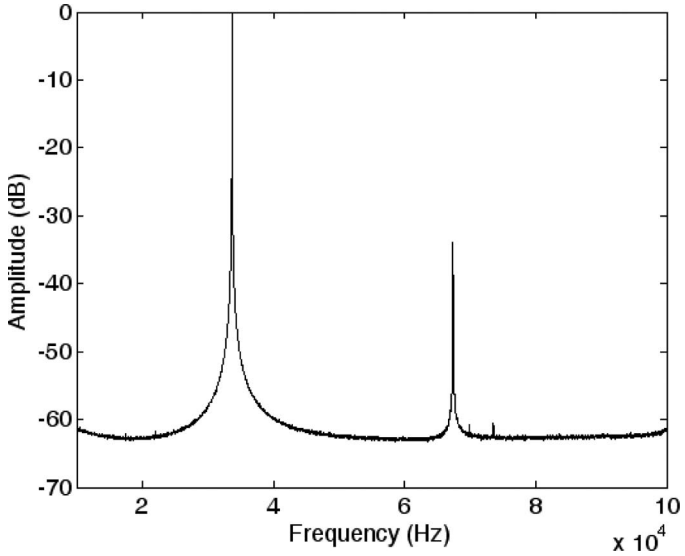

Fig. 9. Frequency spectrum of the average particle velocity for the front face of the 33-kHz Tonpilz device, as measured by the laser vibrometer in air.

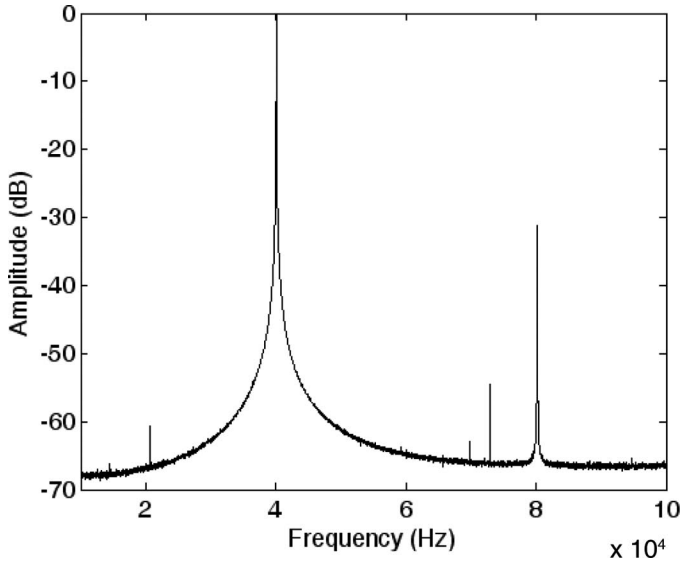

Fig. 10. Frequency spectrum of the average particle velocity for the front face of the 40-kHz Tonpilz device, as measured by the laser vibrometer in air.

motion, the laser vibrometer can also provide an insight in the mechanical behavior at these higher frequencies. From the motion analysis, both the Tonpilz transducers demonstrate reasonably uniform motion across the front face at their respective 2nd harmonics (67.4 and 80.2 kHz, respectively). There are several possible reasons for the occurrence of harmonics at such low drive voltages with the Tonpilz devices. The most likely explanation is the construction of the device itself, in which the individual components collide with each other at the resonance frequency as opposed to simply moving as a complete mechanism. Through this, each impact would generate a series of higher harmonics at multiples of the driving frequency Another possible explanation is the formation of a standing wave within the center bolt, because it acts like a closed conduit for acoustic energy similar to the operation of an organ pipe. However, the latter would likely be represented in the detailed FEA conducted to simulate the transducer and this nonlinear behavior was not evident in electrical impedance proles. It may also be a function of the piezoelectric ceramic operating under intense compression caused by the torque of the center bolt, but again this is considered unlikely

D. Evaluation of Nonlinearities in a Test Cell

Having completed an experimental investigation eliminating any spurious causes for nonlinearity that cannot be attributed to the transmission load, it is necessary to evaluate the linearity of both high-power systems operating with degassed water load. Because of the dicultyin inserting a conventional probe into the system and subsequent problems in positional manipulation for accurate spatial alignment, a membrane hydrophone was selected as the most suitable measurement device. This oered the advantage of simple insertion (only a connecting wire need be fed out from the cell) but also reliable spatial positioning, because the active element could be placed in the center of the cell through design. The type of device employed is a simple single-layer PVDF membrane with a 5-mm active element in the center and an outer diameter equal to that of the cell interior. Because of the relative nature of the measurements required, i.e., amplitude of 2nd harmonic to fundamental, the device was not calibrated. Furthermore, the hostile nature of measurement environment ensured a short operational life of the membrane because of electrode degradation caused by inertial cavitation. It was not deemed necessary to expend resources (time and expense because of the added complexity required) to protect the device from these eects because the experiment did not require long-term use of the hydrophone.

The experimental drive equipment remained consistent with previous measurements. Input voltage was ramped steadily from 50 to 250 mV (15 V to 80 V output), at which point the output voltage from the hydrophone exceeded the maximum for accurate scope measurements. Importantly, no pre-amplier stage was used. The membrane hydrophone was tted into the cell using thin aluminum holders xed onto the aluminum holder ring; these stabilize the position of the device in the center of the cell with the active element along the acoustic axis.

It is important to note that at the upper voltage range signicant levels of cavitation are clearly evident, with jetting and sub-harmonics of the bubble collapses throughout the system visible and audible to the observer. Fig. 11 shows a picture of the degraded electrode connection after short exposures to the cavitational eects in both systems. Moreover, these eects became apparent at lower input levels of approximately 130 mV (41 V output) for the 33-kHz Tonpilz device and 150 mV (48 V output) for the 40-kHz Tonpilz. This is due to increased output from the 33-kHz device comparatively [21], and the longer

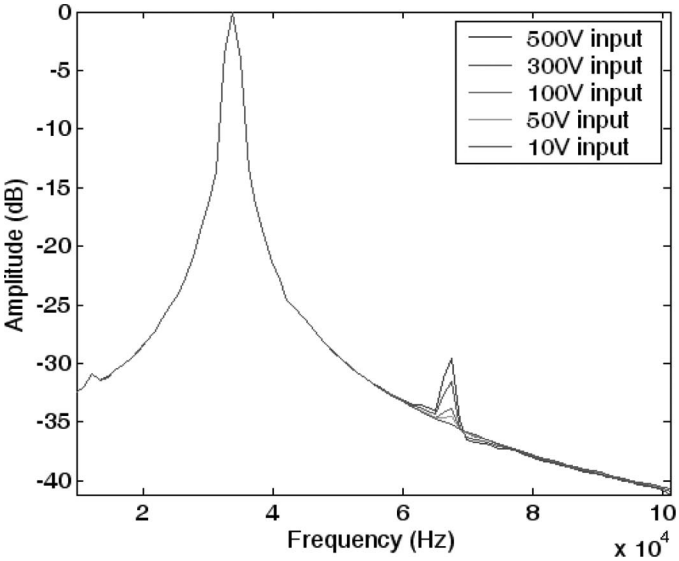

Fig. 14. FFT of pressure at maximum pressure point on the axial plane of the 33-kHz system for increasing voltage input levels.

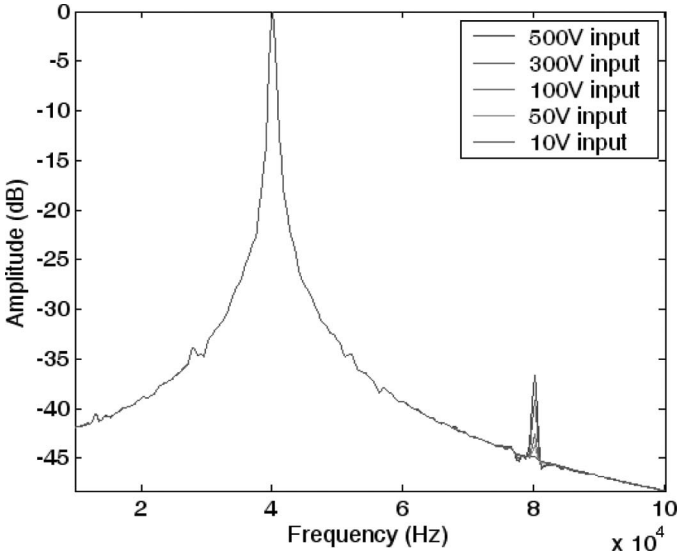

Fig. 15. FFT of pressure at maximum pressure point on the axial plane of the 40-kHz system for increasing voltage input levels.

monic content. This was implemented across the range of input levels.

Figs. 14 and 15 present the frequency spectra across selected input levels for the 33- and 40-kHz systems respectively. For the 33-kHz system, 2nd harmonic presence is initiated at an input voltage of 50 V and is progressively increased to 500 V. However, the peak value of the nonlinear component only surpasses the 30 dB threshold by 1 dB at the highest drive levels. In practice, utilizing this level of input is unlikely and counter-productive because the level of cavitation generated at the transducer front face would negate the efficient transfer of energy into the load as the bubbles disperse the acoustic energy near the radiating aperture. This is mirrored in the frequency response of the 40-kHz system but with lower 2nd harmonic levels reached in general. Crucially, these levels of harmonic activity are comparable with those measured in Sections III-C and III-D, where the 40-kHz system demonstrates a lower 2nd harmonic level than the 33-kHz system.

Therefore, through a combination of experimental and simulated results it can be stated that high-power systems similar to this configuration do not generate nonlinear propagation effects in the transmission load at input levels that are large enough to stimulate cavitational effects in the load, where the measurement threshold for nonlinearity is taken as 30 dB.

IV. D

In many applications, cavitational activity is not usually measured directly, rather the influence of the cavitating field on the load medium (i.e., the reaction itself) is used to define the system performance. In general, this is considered a reasonable assumption from an end user's perspective, but may result in inefficient ultrasonic systems, especially when considering complex reactor designs and large-scale reactor systems. There have been several reviews of high-power ultrasonic applications in recent years [22]–[24], which serve to illustrate the significant advances made in this area. One major concern is the design and development of efficient ultrasonic reactors, in particular related to large-scale operation [22], [23]. Thus, it is important to utilize appropriate design tools to ensure that future ultrasonic reactors will operate in an efficient manner with respect to power considerations and also provide good system performance in terms of process intensification. This work has served to demonstrate that a finite element simulation approach can be exploited for this purpose; PZFlex has been utilized in this work. Thus, FE techniques can be used to develop efficient transduction configurations within high-power ultrasonic reactor vessels and importantly target the design toward a desired cavitation field distribution within the vessel itself.

The results presented in this paper are also important in terms of characterization of a high-power ultrasonic system. There are few options currently available for the measurement of a cavitating ultrasonic field, with the NPL cavitation sensor [25] and fiber optic techniques [26], [27] generally accepted as the most appropriate. The hypothesis presented here that these high-power ultrasonic systems are inherently linear up to the onset of cavitation substantiates the reactor characterization approach previously adopted by the authors [6], [21] in which the pressure field measurement is conducted at low power levels and used to indicate the location of cavitation hot spots in the system.

The implication for the design of future ultrasonic systems is that the simulation, design, and field characterization can be conducted in the low-power regime using conventional techniques. This has the advantage of quantifying the efficiency of new ultrasonic reactor designs in terms of percentage coverage of the cavitation within the vessel

reactor and transfer of energy from the ultrasonic transducer into the load medium. Notwithstanding, there will still be a requirement to measure the extent of cavitation on the process under investigation, and therefore, the conventional physical [25]–[27] and chemical [28] techniques will still be essential for the end-user communities.

V. Conclusion

An introduction to classical nonlinear propagation with reference to high-power cells has been described in this paper. The hypothesis proposed contradicts the commonly held perception that these systems are highly nonlinear before cavitation occurs and therefore, linear models for predicting regions of high pressure are invalid. A review of the common nonlinear models is presented, each accompanied with a brief synopsis of the merits and limitations of each. The most comprehensive analytical nonlinear model is a time- or frequency-domain solution to the KZK equation, although it is decient when representing focused sources and medium inhomogeneities. Given this, a numerical solution to the problem was considered using transient FEA software capable of modeling nonlinear propagation. The FEA code allows for small, incremental linear solutions to be culminated over time, providing an accurate solution to nonlinear problems. The PZFlex code was utilized to investigate the nonlinear behavior associated with the low-frequency Tonpilz devices in a high-power setting.

Spectral analysis was performed on the associated equipment to isolate any effects of equipment nonlinearity from those occurring in the transmission load. Equipment nonlinearity was found to be no higher than 40 dB, whereas 2nd harmonic levels in the Tonpilz devices were approximately 30 dB relative to the fundamental amplitude, even at low input levels. Next, a membrane hydrophone was employed to measure nonlinear effects present within the vessel load. Taking into account the intrinsic nonlinearity of the Tonpilz devices, the conventional nonlinear behavior, i.e., steepening of the wave profile, was found to be minimal even when the system was observed to be cavitating. Linearity at these input levels was confirmed via transient FE analysis.

Therefore, it is reasonable to state that these systems are inherently linear in conventional terms, at least up to the onset of cavitation. This facilitates the use of reliable linear models to predict regions of high pressure and where cavitation is likely to occur in such systems. Consequently, any measurement technique applied at low input levels will accurately represent the field profile until cavitation begins.

A

The authors acknowledge funding for this research through EPSRC projects EP/F016522/1 and EP/N17928/01. Furthermore, the authors thank the reviewers for their efforts and comments that undoubtedly helped improve the quality of this manuscript for publication.

R

[1] M. J. W. Povey and T. J. Mason, *Ultrasound in Food Processing*. London, UK: Blackie Academic and Professional, 1998.

[2] H. Jokonen, P. Pirknon, M. Nystrom, J. Nuortila-Jokinen, and A. Conroos, "Experimental aspects of ultrasonically enhanced cross-flow membrane filtration of industrial wastewater," *Ultrason. Sonochem.*, vol. 13, no. 4, pp. 295–302, 2006.

[3] P. Piyasena, E. Mohareb, and R. C. McKellar, "Inactivation of microbes using ultrasound: a review," *Int. J. Food Microbiol.*, vol. 87, no. 3, pp. 207–216, 2003.

[4] A. Shoh, "Industrial applications of ultrasound—A review I. High power ultrasound," *IEEE Trans. Ultrason. Ferroelectr. Freq. Control*, vol. 22, no. 2, pp. 60–71, 1975.

[5] F. C. N. Lim, M. P. Cartmell, A. Cardoni, and M. Lucas, "A preliminary investigation into optimising the response of vibrating systems used for ultrasonic cutting," *J. Sound Vibrat.*, vol. 272, no. 3-5, pp. 1047–1069, 2004.

[6] A. Gachagan, A. McNab, R. Blindt, M. Patrick, and C. Marriott, "A high power ultrasonic array based test cell," *Ultrasonics*, vol. 42, no. 1-9, pp. 57–68, 2004.

[7] T. J. Mason, E. Joyce, S. S. Phull, and J. P. Lorimer, "Potential uses of ultrasound in the biological decontamination of water," *Ultrason. Sonochem.*, vol. 10, no. 6, pp. 319–323, 2003.

[8] A. Gachagan, D. Speirs, and A. McNab, "The design of a high power ultrasonic test cell using finite element modelling techniques," *Ultrasonics*, vol. 41, no. 4, pp. 283–288, 2003.

[9] J-L. Laborde, C. Bouyer, J-P. Caltagirone, and A. Gerard, "Acoustic cavitation field prediction at low and high frequency ultrasounds," *Ultrasonics*, vol. 36, no. 1–5, pp. 581–587, 1998.

[10] R. Pecha and B. Gompf, "Microimplosions: Cavitation collapse and shock wave emissions on a nanosecond time scale," *Phys. Rev. Lett.*, vol. 84, no. 6, pp. 1328–1330, 2000.

[11] M. Patrick, R. Blindt, and J. Janssen, "The effect of ultrasonic intensity on the crystal structure of palm oil," *Ultrason. Sonochem.*, vol. 11, no. 3–4, pp. 251–255, 2004.

[12] V. F. Humphrey, "Nonlinear propagation in ultrasonic fields: Measurements, modelling and harmonic imaging," *Ultrasonics*, vol. 38, no. 1–8, pp. 267–272, 2000.

[13] L. Bjorno, "Forty years of nonlinear ultrasound," *Ultrasonics*, vol. 40, no. 1–8, pp. 11–17, 2002.

[14] M. F. Hamilton and D. T. Blackstock, *Nonlinear Acoustics*, New York, NY: Academic Press, 1998.

[15] M. A. Averkiou and M. F. Hamilton, "Nonlinear distortion of short pulses radiated by plane and focused pistons," *J. Acoust. Soc. Am.*, vol. 102, no. 2, pp. 2539–2548, 1997.

[16] M. F. Hamilton and Y. S. Lee, "Time-domain modelling of pulsed finite amplitude sound beams," *J. Acoust. Soc. Am.*, vol. 97, no. 2, pp. 906–917, 1995.

[17] S. I. Aanonsen, T. Barkve, J. Naze Tjotta, and S. Tjotta, "Distortion and harmonic generation in the nearfield of a finite amplitude sound beam," *J. Acoust. Soc. Am.*, vol. 75, no. 3, pp. 749–768, 1984.

[18] N. N. Abboud, G. L. Wojcik, D. K. Vaughan, J. Mould, D. J. Powell, and L. Nikodym, "Finite element modelling for ultrasonic transducers," in *SPIE Int. Symp. Medical Imaging*, 1999, vol. 3341, pp. 19–42.

[19] G. Hayward, G. Benny, R. Banks, and W. Galbraith, "The radiation field characteristics of piezoelectric polymer membrane transducers when operating into air," *IEEE Trans. Ultrason. Ferroelectr. Freq. Control*, vol. 47, no. 6, pp. 1438–1447, 2000.

[20] G. Harvey and A. Gachagan, "Non-invasive field measurement of low-frequency ultrasonic transducers operating in sealed vessels," *IEEE Trans. Ultrason. Ferroelectr. Freq. Control*, vol. 53, no. 10, pp. 1749–1758, 2006.

[21] *Laser Doppler Vibrometer User Manual*, Polytec GmbH, Waldbronn, Germany, 2001, pp. 5-1–5-12.

[22] J. A. Gallego-Juarez, "High-power ultrasonic processing: recent developments and prospective advances," *Proc. Int. Congress on Ultrasound*, vol. 3, no. 1, pp. 35–47, 2009.

[23] M. Lucas, A. Gachagan, and A. Cardoni, "Applications and opportunities in power ultrasonics," *J. Mech. Eng. Sci.*, vol. 223, C12, pp. 2949–2965, 2009.